The Mitotic Function of Augmin is Dependent on Its Microtubule-Associated Protein Subunit EDE1 in Arabidopsis thaliana

Julie Lee, Yuh-Ru; Hiwatashi, Yuji; Hotta, Takashi; Xie, Tingting; Doonan, John; Liu, Bo

Published in:
Current Biology

DOI:
10.1016/j.cub.2017.11.030

Publication date:
2017

Citation for published version (APA):
Julie Lee, Y-R., Hiwatashi, Y., Hotta, T., Xie, T., Doonan, J., & Liu, B. (2017). The Mitotic Function of Augmin is Dependent on Its Microtubule-Associated Protein Subunit EDE1 in Arabidopsis thaliana. *Current Biology*, *27*(24), 3891-3897. [e4]. https://doi.org/10.1016/j.cub.2017.11.030

Current Biology

The mitotic function of augmin is dependent on its microtubule-associated protein subunit EDE1 in Arabidopsis thaliana

--Manuscript Draft--

Manuscript Number:	CURRENT-BIOLOGY-D-17-00762R3
Full Title:	The mitotic function of augmin is dependent on its microtubule-associated protein subunit EDE1 in Arabidopsis thaliana
Article Type:	Report
Corresponding Author:	Bo Liu CA UNITED STATES
First Author:	Bo Liu
Order of Authors:	Bo Liu
	Yuh-Ru Julie Lee
	Yuji Hiwatashi
	Takashi Hotta
	Tingting Xie
	John Doonan
Abstract:	The augmin complex plays an essential role in microtubule (MT)-dependent MT nucleation by recruiting the -tubulin complex to MT walls in order to generate new MTs [1]. The complex contains eight subunits (designated AUG) including AUG8, which is an MT-associated protein (MAP). When this complex is isolated from etiolated seedlings consisting of primarily interphase cells in Arabidopsis thaliana, AUG8 is an integral component [2]. The EDE1 (Endosperm DEfective 1) is homologous to AUG8 [3]. Here we demonstrate that EDE1, but not AUG8, was associated with acentrosomal spindle and phragmoplast MT arrays in patterns indistinguishable from those of the AUG1-7 subunits and the -tubulin complex proteins (GCPs) that exhibited biased localization towards MT minus ends. Consistent with this co-localization, EDE1 directly interacted with AUG6 in vivo. Moreover, a partial loss-of-function mutation, ede1-1, compromised the localization of augmin and -tubulin on the spindle and phragmoplast MT arrays and led to serious distortions in spindle MT remodeling during mitosis. However, mitosis continued even when kinetochore fibers were not obviously discernable and cytokinesis took place following the formation of elongated bipolar phragmoplast MT arrays in the mutant. Hence, we conclude that the mitotic function of augmin is dependent on its MAP subunit EDE1, which cannot be replaced by AUG8, and the cell cycle-dependent function of augmin can be differentially regulated by employing distinct MAP subunits. Our results also illustrate that plant cells can respond flexibly to serious challenges of compromised MT-dependent MT nucleation in order to complete mitosis and cytokinesis.

Dear Dr. Knowlton:

Ref.: Revision of Ms. No. CURRENT-BIOLOGY-D-17-00762R2

We have formatted the manuscript according to the guidelines provided by Current Biology. Please receive the files.

Thank you for your attention.

Sincerely,

Bo Liu

The handling editor Dr. Knowlton has indicated that “We agree that you have addressed the points from the referees, and we are happy to proceed with the paper.”

Cell Press Conflict of Interest Form

If submitting materials via Editorial Manager, please complete this form electronically and upload the file with your final submission.

Otherwise, please return the form as an email attachment to the copyeditor handling your manuscript.

Cell Press requires all authors to disclose any financial interest that might be construed to influence the results or interpretation of their manuscript.

As a guideline, any affiliation associated with a payment or financial benefit exceeding $10,000 p.a. or 5% ownership of a company or research funding by a company with related interests would constitute a financial interest that must be declared. This policy applies to all submitted research manuscripts and review material.

Examples of statement language include: AUTHOR is an employee and shareholder of COMPANY; AUTHOR is a founder of COMPANY and a member of its scientific advisory board. This work was supported in part by a grant from COMPANY.

Please disclose any such interest below on behalf of all authors of this manuscript.

Please check one of the following:

☒ None of the authors of this manuscript have a financial interest related to this work.

☐ Please print the following disclosure statement in the Acknowledgments section:

Please provide the following information:

☒ Please check this box to indicate that you have asked every author of this work to declare any conflicts of interest. Your answers on this form are on behalf of every author of this work.

Manuscript #: 17-00762R2

Title: The mitotic function of augmin is dependent on its microtubule-associated protein subunit EDE1 in Arabidopsis thaliana

Author list: Yuh-Ru Julie Lee, Yuji Hiwatashi, Takashi Hotta, Tingting Xie, John H. Doonan, Bo Liu

Your name: Bo Liu

Date: November 1, 2017

Cell Press, 50 Hampshire Street, 5th floor, Cambridge, MA 02139, USA

Graphical Abstract

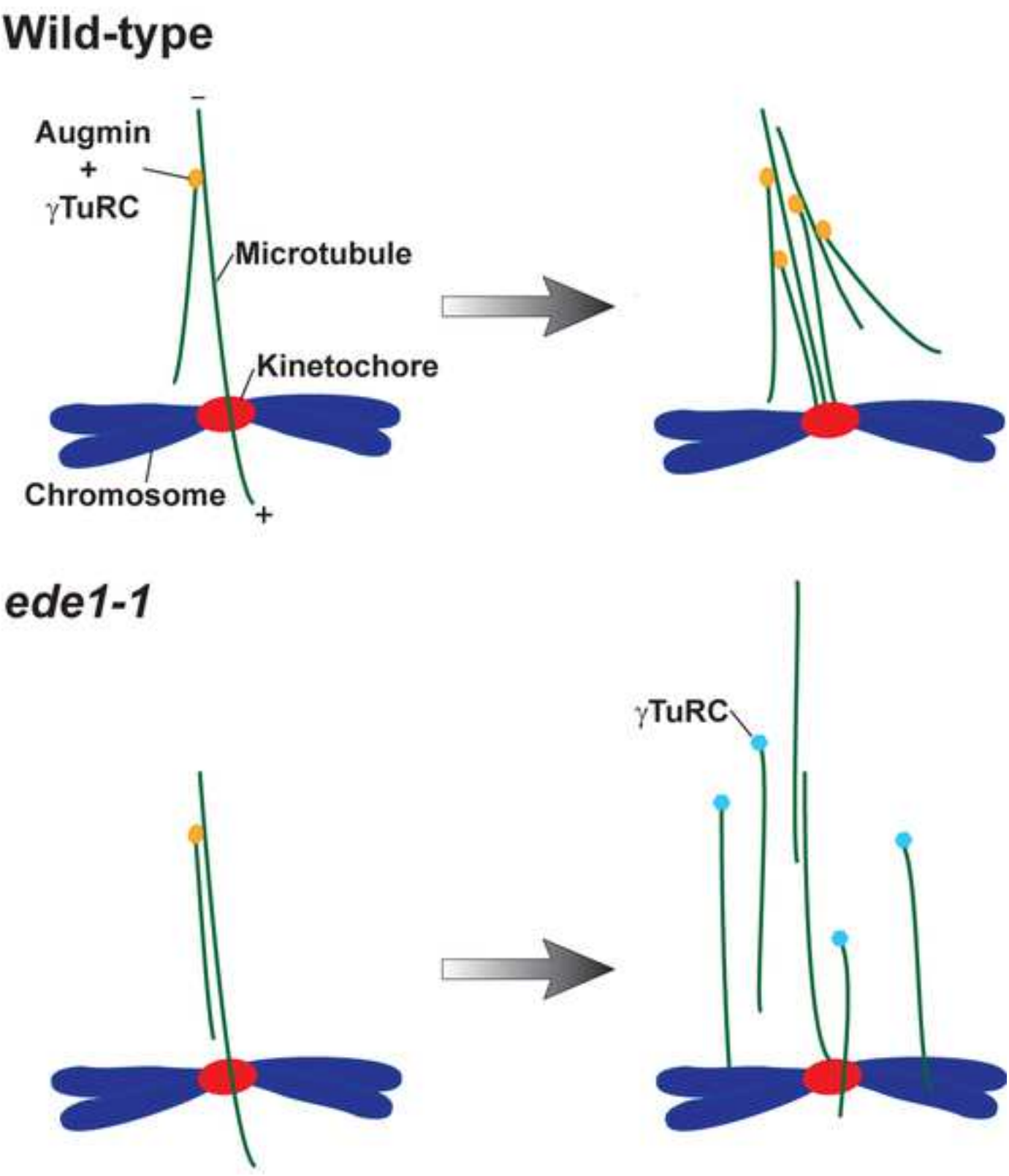

The mitotic function of augmin is dependent on its microtubule-associated protein subunit EDE1 in *Arabidopsis thaliana*

Yuh-Ru Julie Lee[1], Yuji Hiwatashi[2,3], Takashi Hotta[1,4], Tingting Xie[1,5], John H. Doonan[2], Bo Liu[a,6]

[1] Department of Plant Biology, University of California, Davis, CA 95616, USA

[2] The National Plant Phenomics Centre, IBERS, Aberystwyth University, Aberystwyth, SY23 3EB, UK

[3] Current address: School of Food, Agricultural and Environmental Sciences, Miyagi University, Sendai, Miyagi 982-0215, Japan

[4] Current address: Carnegie Institution for Science, Department of Embryology, Baltimore, MD 21218, USA

[5] Current address: College of Life Sciences and Technology, Huazhong Agricultural University, Wuhan, Hubei 430070, China

[6] Lead Contact

Correspondence: bliu@ucdavis.edu (B.L.) & jhd2@aber.ac.uk (J.H.D.)

Running title: M phase specific plant augmin complex

SUMMARY

The augmin complex plays an essential role in microtubule (MT)-dependent MT nucleation by recruiting the γ-tubulin complex to MT walls in order to generate new MTs [1]. The complex contains eight subunits (designated AUG) including AUG8, which is an MT-associated protein (MAP). When this complex is isolated from etiolated seedlings consisting of primarily interphase cells in *Arabidopsis thaliana*, AUG8 is an integral component [2]. The EDE1 (Endosperm DEfective 1) is homologous to AUG8 [3]. Here we demonstrate that EDE1, but not AUG8, was associated with acentrosomal spindle and phragmoplast MT arrays in patterns indistinguishable from those of the AUG1-7 subunits and the γ-tubulin complex proteins (GCPs) that exhibited biased localization towards MT minus ends. Consistent with this co-localization, EDE1 directly interacted with AUG6 *in vivo*. Moreover, a partial loss-of-function mutation, *ede1-1*, compromised the localization of augmin and γ-tubulin on the spindle and phragmoplast MT arrays and led to serious distortions in spindle MT remodeling during mitosis. However, mitosis continued even when kinetochore fibers were not obviously discernable and cytokinesis took place following the formation of elongated bipolar phragmoplast MT arrays in the mutant. Hence, we conclude that the mitotic function of augmin is dependent on its MAP subunit EDE1, which cannot be replaced by AUG8, and the cell cycle-dependent function of augmin can be differentially regulated by employing distinct MAP subunits. Our results also illustrate that plant cells can respond flexibly to serious challenges of compromised MT-dependent MT nucleation in order to complete mitosis and cytokinesis.

RESULTS AND DISCUSSION

EDE1 co-locates with γ-tubulin on spindle and phragmoplast MT arrays

Microtubule (MT)-dependent MT nucleation takes place on the surface of preexisting MTs and makes key contributions to assembling both mitotic and interphase MT arrays [1]. In cells of flowering plants that lack structurally defined MT-organizing centers, this mode of MT generation becomes particularly prominent [4]. MT nucleation depends on the γ-tubulin ring complex (γTuRC) which serves as a template for initiating new MT polymerization and caps the MT minus end [5]. The augmin protein complex recruits the γTuRC to extant MTs in order to initiate MT-dependent MT nucleation [1]. In plants, mutations that compromise the function of augmin often lead to the collapse of both the spindle and phragmoplast MT arrays [2, 6, 7]. In the model *Arabidopsis thaliana*, the AUG8 subunit of augmin was predicted to be an MT-associated protein (MAP) based on its high isoelectric point (PI) (> 10) while other AUG subunits are rather acidic [2]. Previously, we have demonstrated that AUG1-7 subunits exhibit similar localization patterns on spindle and phragmoplast MTs, biasing towards their minus ends in a pattern indistinguishable from that of the γTuRC [2, 6]. However, AUG8 was not detected on spindle or phragmoplast MTs and *aug8* loss-of-function mutations did not cause noticeable phenotypes in cell division and plant growth (data not shown). But AUG8 interacted with the rest of the augmin complex *in vivo* as demonstrated by co-purification (data not shown). Therefore, we were intrigued by this discrepancy in localizations of AUG8 and other augmin subunits.

In *A*. *thaliana*, AUG8 is one of nine members of a QWRF motif-containing protein family, including EDE1 (Endosperm DEfective 1) and SCO3 (Snowy Cotyledon 3) [3, 8]. Because augmin is essential but the earlier isolated AUG8 subunit is dispensable for mitosis and cytokinesis in *A*. *thaliana*, we went on to test whether an AUG8 homolog would replace AUG8 for these important processes. *EDE1* is an essential gene encoding a MAP as determined by an *in vitro* MT co-sedimentation assay and exhibits a cell cycle-dependent expression pattern regulated by the transcriptional DREAM complex [3, 9]. The sequence similarity among AUG8, EDE1, SCO3 and other proteins in this family suggests that different isoforms are differentially utilized to assemble augmin complexes in a spatially or temporally regulated manner. The *ede1-1* mutation, located at an intron-exon splicing junction leads to the production of a truncated EDE1 protein with deletion of 18 amino acids [3]. The mutant produces expanded leaves, indicating that MT activities at interphase are not seriously affected. To test whether EDE1 was associated with MT arrays during mitosis, a GFP-EDE1 was expressed under the control of its native promoter in this partial loss-of-function mutant. GFP-EDE1 expression fully suppressed the defects in seed morphology and root growth brought about by the mutation (Figure1), indicating that the fusion protein was functional. We examined cycling cells in the root meristem and found that GFP-EDE1 associated with MT arrays during mitosis (Figure 1A; Movie 1S). It became concentrated towards the poles at late prophase before nuclear envelope broke down. The signal became more conspicuous on the spindle as the typical bipolar spindle morphology developed. A dark spindle midzone became wider, concomitantly with progression through anaphase (Figure 1A, from 9:36 to 11:24). The signal became particularly prominent at spindle poles towards the end of anaphase (Figure 1A, at 11:24). Upon completion of anaphase, GFP-EDE1 started to accumulate in the spindle midzone in two halves, flanking

a central dark zone (Figure 1A, at 13:48). GFP-EDE1 gradually became concentrated towards the center as the phragmoplast developed, and decorated the phragmoplast as it expanded towards the cell cortex (Figure 1A, from 14:24 to 28:48).

To demonstrate the relationship between EDE1 and mitotic MT arrays, GFP-EDE1 and MTs were labeled in fixed meristematic cells by using anti-GFP and anti-tubulin DM1A antibodies, respectively. Prior to nuclear envelope breakdown when the preprophase band MTs were still visible, GFP-EDE1 was concentrated near the future spindle poles (Figure1B). Later, EDE1 became enriched in the spindle apparatus with MT bundles and co-colocalized with phragmoplast MTs as well (Figure 1B). Furthermore, the GFP-EDE1 signal was highly coincident with that of γ-tubulin, as revealed by the monoclonal G9 antibody [10], and the augmin subunit AUG3 as demonstrated in fixed and living cells, respectively (Figure S2). Therefore, we concluded that GFP-EDE1 exhibited a localization pattern similar to those of AUG1-7 and the γTuRC.

Both AUG8 and EDE1 direct the augmin complex to MTs

To test whether EDE1, in comparison to AUG8, interacted with other augmin subunit(s), we co-expressed AUG8 or EDE1 with other AUG subunits in tobacco leaf epidermal cells using the strong viral 35S promoter. Therefore the proteins were produced in vast excess over the amount that might be incorporated into the tobacco augmin complex, thus freeing up the great majority of the proteins to express their interactive properties. First, we examined the localization patterns of each AUG subunit expressed alone and found that only AUG8 decorated the endogenous cortical MTs highlighted by the MT-marker CTD-RFP (Figure S3A). Although the animal counterpart of AUG6 has been shown to bind to MTs *in vitro* [11], AUG6 exhibited a diffuse localization pattern in the cytoplasm (Figure S3A). However, when AUG6 was co-expressed with AUG8, AUG6 was then recruited to cortical MTs (Figure S3B). When the other 6 subunits were co-expressed with AUG8, they remained diffuse in the cytosol (Figure S3B). Therefore, we concluded that the AUG8 subunit interacts with AUG6 and we deduce that the same interaction occurs in the assembled augmin complex as well. To test whether EDE1 behaves like AUG8 and recapitulates the interaction with AUG6 *in vivo*, we expressed EDE1 alone and detected it on cortical MTs (Figure 2A), confirming its MT-association activity as indicated by *in vitro* MT-co-sedimentation assays [3]. When co-expressed with EDE1, AUG6 was recruited to cortical MTs and the two fusion proteins overlapped completely (Figure 2B-2D). Therefore, we concluded that, upon expression in interphase cells, EDE1 interacted with cortical MTs and recruited AUG6, likely by direct interaction. AUG8/EDE1-dependent AUG6 recruitment to MTs is most likely important for the localization of the entire augmin complex and consequently could direct the γTuRC to the flanks of MTs, including spindle and phragmoplast MTs.

To directly test whether EDE1 was present in complex(es) with other AUG subunits, we expressed GFP-EDE1 under the control of the viral 35S promoter in transgenic *A*. *thaliana* plants. GFP-EDE1 was purified by using an anti-GFP affinity column. When the purified proteins were analyzed by mass spectrometry-assisted peptide identification, AUG3, AUG4, AUG5, AUG6, and AUG7 were co-purified with peptide coverages from 7.33% to 26.14% (Figure 2E). None of these subunits was detected in a control experiment when the Kinesin-4A/FRA1-GFP was used as the bait (data not shown), indicating

that the association of GFP-EDE1 with other augmin subunits was specific. We did not detect AUG1 and AUG2 in this experiment, perhaps because of the lower recovery of the augmin complex by using GFP-EDE1 as the bait when compared to employing AUG3-GFP as the bait. Nevertheless, we concluded that EDE1 indeed was incorporated into the augmin complex as an integral subunit in interphase cells when ectopically expressed.

EDE1 is required for normal spindle and phragmoplast MT reorganization

To understand how the EDE1 protein contributed to MT organization and function during mitosis, we exploited the partial loss-of-function mutant *ede1-1*, which strongly depresses the production of full length transcript, comparing MT organization in mutant and control plants using the GFP-TUB6 (β-tubulin 6) as a marker (Movies S2 and S3). In the control cells, MTs were coalesced and quickly appeared in conspicuous bundles following nuclear envelope breakdown (Figure 3A, -6:54). Soon after kinetochore MT fibers became prominent, highlighting chromosome congression at the metaphase plate (Figure 3A, 0:0). This was followed by orchestrated shortening of kinetochore fibers at anaphase and rapid polymerization of new MTs in the spindle midzone (Figure 3A, 0:54 to 2:24). These spindle midzone MTs were organized into two mirrored halves with a dark line of much reduced fluorescence in the middle, marking the birth of the phragmoplast MT array (Figure 3A, 3:18 to 5:06). The MTs in this array soon had shortened so that its axial width became reduced, and in the meantime the array expanded in the horizontal direction towards the parental cell membrane (Figure 3A, 5:06 to 14:06). These aspects of MT reorganization were greatly affected in the *ede1-1* mutant cells. First of all, MTs were organized into skewed and greatly elongated bundles following the nuclear envelope breakdown (Figure 3B, -7:30 to -1:48). While more MTs were added as indicated by some prominent MT bundles, no obvious metaphase plate was established (Figure 3B, 0:0). These much elongated MT bundles underwent reorganization with the fluorescent signal gradually increased towards the two poles as if MTs exhibited poleward sliding (Figure 3B, 0:36 to 1:48). Later, the spindle midzone became noticeable and more MTs joined the initial thin bundles and a dark line with dimmed fluorescence emerged, indicating the establishment of the bipolar phragmoplast MT array (Figure 3B, 3:36 to 5:24). An obvious difference between the phragmoplast MT arrays in *ede1-1* vs. control cells was that the axial width of the array became wider in the mutant cells during the expansion of the array (Figure 3B, 5:24 to 11:42). Therefore, both spindle and phragmoplast MT arrays were seriously challenged by the *ede1-1* mutation in terms of both morphology and orientation. In spite of the distortion of MT arrays, the mutant cells managed to complete the entire process of mitosis and cytokinesis reasonably well so that seedlings could be reproduced from generation to generation.

EDE1 is necessary for augmin localization to mitotic arrays

We next asked whether the distorted MT reorganization patterns were due to altered localization of augmin and/or γTuRC in the *ede1-1* mutant cells. To answer this, AUG3 and γ-tubulin localizations were determined by immunofluorescence. First AUG3-GFP, a functional fusion as tested previously [6], was expressed in the *ede1-1* mutant and the meristematic cells of the resulting transgenic plants were processed for anti-GFP staining. In contrast to the control cells in which AUG3-GFP exhibited conspicuous colocalization with spindle and phragmoplast MTs (Figure S2), AUG3-GFP was largely

diffuse within the *ede1-1* cytosol in both a metaphase-like cell and one bearing elongated phragmoplast MT array (Figure S4A). AUG3-GFP signal was essentially absent or much reduced on MT bundles in both spindle and phragmoplast.

When γ-tubulin was localized in *ede1-1* mitotic cells using the G9 antibody, its enrichment at the poles of the pro-spindle towards the end of prophase was discerned albeit without forming striking polar caps (Figure 4) and intensified signals were also detected among MTs on the nuclear envelope at this stage. In metaphase-like cells, γ-tubulin signal became evenly distributed in the cytosol (Figure 4). In contrast to control cells where γ-tubulin was largely detected on phragmoplast MTs, *ede1-1* cells did not show obvious concentration of γ-tubulin on the phragmoplast MT array (Figure 4). A particularly noticeable difference compared to the control cells was that γ-tubulin accumulated on the reforming nuclear envelope during cytokinesis (Figure 4). Its presence there perhaps would initiate new MT nucleation towards the end of cytokinesis.

Cell cycle-dependent augmin function

To determine if EDE1 and AUG8 are differentially employed for the assembly of the augmin complex in mitotic vs. interphase cells, we performed augmin complex purification (a) from young flower buds enriched with actively cycling cells and (b) from expanded leaves with largely differentiating or differentiated cells. When AUG3-GFP was used as the bait, AUG1-7 were purified at comparable yields based on the numbers of peptides identified by mass spectrometry (Figure 2E, Talbe S3-4). While both AUG8 and AUG8Like (AUG8L) were detected under both circumstances, EDE1 was only detected from the preparation from young flower buds (Figure 2E, Talbe S3-4). This result shows that the EDE1 protein is part of the augmin complex in proliferating tissues but cannot be detected in the augmin complexes of differentiated tissues. Taken together with EDE1 localization at the cellular level, this data strongly indicates that the mitotic function of augmin depends on EDE1.

We then asked whether the EDE1 function could be replaced by AUG8 when the latter assumed the EDE1 expression pattern. We used the *EDE1* promoter which was used for the *ede1-1* rescue experiment to drive the expression of GFP-AUG8. First, we asked whether this ectopically expressed GFP-AUG8 fusion protein became associated with the spindle apparatus. Compared to GFP-EDE1 which was detected on a metaphase spindle, GFP-AUG8 localized along spindle MTs (Figure S4A-B). Then we examined the functionality of the fusion protein. While the spindle elongation phenotype caused by the *ede1-1* mutation was rescued by the expression of GFP-EDE1, it was not so in two independent lines expressing GFP-AUG8 under the control of the *EDE1* promoter (Figure S4C). Therefore, we conclude that the mitotic function of augmin required unique features of EDE1 which are determined by its amino acid sequence.

Collectively, our results demonstrate that the cell cycle-dependent function of augmin is dependent on the EDE1 protein, which acts as the MAP subunit of the complex during mitosis in *A. thaliana*. EDE1, AUG8, AUG8L, and six other proteins share the signature amino acid motif "QWRF" residues [3, 8]. Evolutionary divergence within the family is further evidenced by the low level of sequence homology with the three examined members, EDE1, SCO3 and AUG8, exhibiting nearly no sequence homology in

their N-termini while the C-termini showed limited conservation [3]. Because MT-binding domains typically are basic and bear positive charges, we predicted that the N-terminal half harbors an MT-binding site because of abundant presence of the arginine residues. The MAP subunit of the human augmin also forms an MT-binding site towards the N-terminus [12]. Conversely, the more conserved C-terminal half of EDE1 perhaps forms a binding site for AUG6 so that a functional augmin complex could be assembled for spindle and phragmoplast MT arrays, a scenario resembling the interaction between the human Hice1 and HAUS6 [13].

We hypothesize three scenarios that may reflect the significance of the great divergence of the N-terminal domain of the AUG8/EDE1/QWRF family proteins. First, the divergent sequences may facilitate selective or preferential binding to particular MT arrays at different times. Consequently, augmin complexes utilizing different AUG8 isoforms would be assembled on different MT arrays. Second, such sequence divergence may lead to conformational difference among the proteins so that they could influence MT-branching angles after the augmin complexes are associated with the wall of MTs and recruit the γTuRC. This may be related to the MT nucleation angle at ~40° seen in interphase MT array as demonstrated in *A*. *thaliana* leaf cells [14] and that at <30° in M phase MT arrays as revealed in the frog egg system and human cells [15, 16]. For example, the EDE1-bearing augmin may be responsible for generating MTs with shallow angles and AUG8-included augmin for generating new MTs at ~40° in interphase. Whether EDE1 is required for generating new MTs in parallel to the mother MTs, a phenomenon depending on augmin as well [14], is an open question. The last possibility is that these isoforms may be regulated differentially by posttranslational modifications like phosphorylation. This hypothesis is inspired by the findings that phosphorylation of HICE1, the human counterpart of the AUG8 subunit, by Aurora A and/or the Polo-like Plk1 kinases directly impacts the association of Hice1 with MTs and consequently critical for intraspindle MT nucleation and assembly of the spindle MT array [17, 18]. Although plant genomes do not encode obvious homologs of Plk kinases, the Aurora and NIMA-related NEK kinases in addition to the CDK kinase could phosphorylate EDE1 in order to regulate its activities. In fact, EDE1 is a CDK substrate [19]. Furthermore, the predicted role of Aurora is supported by the fact that the class α Aurora kinase exhibits a localization pattern indistinguishable from that of γ-tubulin in the spindle but not the phragmoplast [20, 21]. In *A*. *thaliana*, there are seven NEK kinases that are involved in MT organization, perhaps by phosphorylating MAPs or even tubulins [22-24]. At least one of them, NEK6 exhibits colocalization with the γ-TuRC-associated WD40 protein NEDD1 [25]. However, it is worth testing whether EDE1 and other AUG8 family proteins are substrates of these different kinases.

Our results also show that, despite the fact that the majority of augmin and γTuRC complexes were no longer associated with spindles and phragmoplasts in the *ede1-1* mutant, MTs underwent continuous reorganization, albeit in twisted patterns, and cell division was largely successful. This contrasted the *aug7* mutant in which γ-tubulin also became diffusely located and phragmoplast MT arrays often collapse so that the plant is dwarf and sterile [2]. However, the null *ede1-3* mutant is early embryo lethal due to failures in cell division [3], further supporting the idea that the mitotic function of augmin

is dependent on EDE1. In the *ede1-1* mutant, the augmin function was compromised so that MTs generated from the wall of extant MTs were greatly reduced because of weakened recruitment of other augmin subunits caused by reduced EDE1-AUG6 interaction. This notion is supported by the observation that elevated expression of the mutant form of EDE1, due to the loss of three repressive MYB3R transcriptional factors, can significantly suppress cell division defects caused by the *ede1-1* mutation alone [9]. We hypothesize, based on the microtubule nucleation function of augmin, that the morphological alteration in spindle and phragmoplast MT arrays in *ede1-1* were caused by changes in MT nucleation patterns. In control cells, it is postulated that MT nucleation was largely represented in branched forms that led to the formation of fir-tree-like kinetochore fibers (Figure S4D). In the *ede1-1* mutant, however, branched nucleation could likely have been compromised while parallel nucleation as well as nucleation events not associated with extant MTs became more represented. Motor driven MT sliding, although without direct evidence currently, may cause spindle MT arrays to be elongated (Figure S4D). Nevertheless, altered MT nucleation, albeit being not so robust, was sufficient to drive cell division forward.

In summary, we present evidence for an M phase specific augmin complex in plants. We hypothesize that the interphase and M phase functions of the augmin complex may be separated through the assembly of complexes utilizing different isoforms in the AUG8 family.

AUTHOR CONTRIBUTIONS

Conceptualization, Y.J.L., Y.H., T.H., J.H.D., and B.L.; Investigation, Y.J.L., Y.H., T.H., and T.X.; Writing-Original Draft, Y.J.L., and B.L.; Writing- Review & Editing, Y.J.L., Y.H., T.H., J.H.D., and B.L.; Visualization, Y.J.L., T.H., and B.L.; Supervision, J.H.D., and B.L.; Funding Acquisition, Y.J.L., Y.H., J.H.D., and B.L.

ACKNOWLEDGEMENTS

We want to thank members of our laboratories for critical comments on the manuscript. Special thanks go to Dr. Jung-Youn Lee at the University of Delaware of the generous gift of the CTD-RFP plasmid, Dr. Tetsuya Horio at Nippon Sport Science University for the G9 antibody, and Dr. Tsuyoshi Nakagawa at Shimane University in Japan for kindly providing the pGWB vectors. This work was supported by the National Science Foundation of USA under the Grant MCB-1412509 to BL and YRL, BBSRC grant BB/D52189X/1 and EU FP7- network grant “AGRON-OMICS” number 37704 to JHD, and European Commission FP7 Marie Curie Fellowship 275257 to YH. Any opinions, findings, and conclusions or recommendations expressed in this material are those of the authors and do not necessarily reflect the views of the funding agencies.

REFERENCES

1. Sanchez-Huertas, C., and Luders, J. (2015). The augmin connection in the geometry of microtubule networks. Curr Biol *25*, R294-299.
2. Hotta, T., Kong, Z., Ho, C.M., Zeng, C.J., Horio, T., Fong, S., Vuong, T., Lee, Y.R., and Liu, B. (2012). Characterization of the Arabidopsis augmin complex uncovers its critical function in the assembly of the acentrosomal spindle and phragmoplast microtubule arrays. Plant Cell *24*, 1494-1509.
3. Pignocchi, C., Minns, G.E., Nesi, N., Koumproglou, R., Kitsios, G., Benning, C., Lloyd, C.W., Doonan, J.H., and Hills, M.J. (2009). ENDOSPERM DEFECTIVE1 Is a Novel Microtubule-Associated Protein Essential for Seed Development in Arabidopsis. Plant Cell *21*, 90-105.
4. Hashimoto, T. (2013). A ring for all: γ-tubulin-containing nucleation complexes in acentrosomal plant microtubule arrays. Curr Opin Plant Biol *16*, 698-703.
5. Kollman, J.M., Merdes, A., Mourey, L., and Agard, D.A. (2011). Microtubule nucleation by γ-tubulin complexes. Nat Rev Mol Cell Biol *12*, 709-721.
6. Ho, C.M., Hotta, T., Kong, Z., Zeng, C.J., Sun, J., Lee, Y.R., and Liu, B. (2011). Augmin plays a critical role in organizing the spindle and phragmoplast microtubule arrays in Arabidopsis. Plant Cell *23*, 2606-2618.
7. Nakaoka, Y., Miki, T., Fujioka, R., Uehara, R., Tomioka, A., Obuse, C., Kubo, M., Hiwatashi, Y., and Goshima, G. (2012). An inducible RNA interference system in Physcomitrella patens reveals a dominant role of augmin in phragmoplast microtubule generation. Plant Cell *24*, 1478-1493.
8. Albrecht, V., Simková, K., Carrie, C., Delannoy, E., Giraud, E., Whelan, J., Small, I.D., Apel, K., Badger, M.R., and Pogson, B.J. (2010). The cytoskeleton and the peroxisomal-targeted snowy cotyledon3 protein are required for chloroplast development in Arabidopsis. Plant Cell *22*, 3423-3438.
9. Kobayashi, K., Suzuki, T., Iwata, E., Nakamichi, N., Suzuki, T., Chen, P., Ohtani, M., Ishida, T., Hosoya, H., Muller, S., et al. (2015). Transcriptional repression by MYB3R proteins regulates plant organ growth. EMBO J *34*, 1992-2007.
10. Horio, T., Basaki, A., Takeoka, A., and Yamato, M. (1999). Lethal level overexpression of γ-tubulin in fission yeast causes mitotic arrest. Cell Motil Cytoskeleton *44*, 284-295.
11. Zhu, H., Coppinger, J.A., Jang, C.Y., Yates, J.R., 3rd, and Fang, G. (2008). FAM29A promotes microtubule amplification via recruitment of the NEDD1-γ-tubulin complex to the mitotic spindle. J Cell Biol *183*, 835-848.
12. Wu, G., Lin, Y.T., Wei, R., Chen, Y., Shan, Z., and Lee, W.H. (2008). Hice1, a novel microtubule-associated protein required for maintenance of spindle integrity and chromosomal stability in human cells. Mol Cell Biol *28*, 3652-3662.
13. Hsia, K.C., Wilson-Kubalek, E.M., Dottore, A., Hao, Q., Tsai, K.L., Forth, S., Shimamoto, Y., Milligan, R.A., and Kapoor, T.M. (2014). Reconstitution of the augmin complex provides insights into its architecture and function. Nat Cell Biol *16*, 852-863.
14. Liu, T., Tian, J., Wang, G., Yu, Y., Wang, C., Ma, Y., Zhang, X., Xia, G., Liu, B., and Kong, Z. (2014). Augmin triggers microtubule-dependent microtubule nucleation in interphase plant cells. Curr Biol *24*, 2708-2713.
15. Petry, S., Groen, A.C., Ishihara, K., Mitchison, T.J., and Vale, R.D. (2013). Branching microtubule nucleation in Xenopus egg extracts mediated by augmin and TPX2. Cell *152*, 768-777.
16. Kamasaki, T., O'Toole, E., Kita, S., Osumi, M., Usukura, J., McIntosh, J.R., and Goshima, G. (2013). Augmin-dependent microtubule nucleation at microtubule walls in the spindle. J Cell Biol *202*, 25-33.

17. Johmura, Y., Soung, N.K., Park, J.E., Yu, L.R., Zhou, M., Bang, J.K., Kim, B.Y., Veenstra, T.D., Erikson, R.L., and Lee, K.S. (2011). Regulation of microtubule-based microtubule nucleation by mammalian polo-like kinase 1. Proc Natl Acad Sci U S A *108*, 11446-11451.
18. Tsai, C.Y., Ngo, B., Tapadia, A., Hsu, P.H., Wu, G., and Lee, W.H. (2011). Aurora-A phosphorylates Augmin complex component Hice1 protein at an N-terminal serine/threonine cluster to modulate its microtubule binding activity during spindle assembly. J Biol Chem *286*, 30097-30106.
19. Pignocchi, C., and Doonan, J.H. (2011). Interaction of a 14-3-3 protein with the plant microtubule-associated protein EDE1. Ann Bot *107*, 1103-1109.
20. Demidov, D., Van Damme, D., Geelen, D., Blattner, F.R., and Houben, A. (2005). Identification and dynamics of two classes of aurora-like kinases in Arabidopsis and other plants. Plant Cell *17*, 836-848.
21. Petrovska, B., Cenklova, V., Pochylova, Z., Kourova, H., Doskocilova, A., Plihal, O., Binarova, L., and Binarova, P. (2012). Plant Aurora kinases play a role in maintenance of primary meristems and control of endoreduplication. New Phytol *193*, 590-604.
22. Motose, H., Hamada, T., Yoshimoto, K., Murata, T., Hasebe, M., Watanabe, Y., Hashimoto, T., Sakai, T., and Takahashi, T. (2011). NIMA-related kinases 6, 4, and 5 interact with each other to regulate microtubule organization during epidermal cell expansion in Arabidopsis thaliana. Plant J *67*, 993-1005.
23. Takatani, S., Otani, K., Kanazawa, M., Takahashi, T., and Motose, H. (2015). Structure, function, and evolution of plant NIMA-related kinases: implication for phosphorylation-dependent microtubule regulation. J Plant Res *128*, 875-891.
24. Vigneault, F., Lachance, D., Cloutier, M., Pelletier, G., Levasseur, C., and Seguin, A. (2007). Members of the plant NIMA-related kinases are involved in organ development and vascularization in poplar, Arabidopsis and rice. Plant J *51*, 575-588.
25. Motose, H., Tominaga, R., Wada, T., Sugiyama, M., and Watanabe, Y. (2008). A NIMA-related protein kinase suppresses ectopic outgrowth of epidermal cells through its kinase activity and the association with microtubules. Plant J *54*, 829-844.

FIGURE LEGENDS

Figure 1. Localization of EDE1 in mitotic cells. (A) Redistribution of GFP-EDE1 during mitosis in an *A. thaliana* root cell as observed by confocal microscopy. Snapshots of GFP-EDE1 following nuclear envelope breakdown (time 0) until late cytokinesis. The GFP signal first appeared towards the spindle poles (1:12, minutes : seconds) and quickly highlights the developing kinetochore fiber MTs (1:48 to 6:36). Following the shortening of kinetochore fibers in anaphase, the GFP-EDE1 signal continued to be associated with the kinetochore fiber MTs and becomes particularly conspicuous at spindle poles towards the end of anaphase (11:24). It appeared in the spindle midzone during telophase (13:48), leaving a wide dark gap in the middle. The signal is associated with developing phragmoplast in two halves (14:24 to 28:48). (B) Dual localizations of GFP-EDE1 and MTs by immunofluorescence in three representative stages of the cell division cycle. In merged images, GFP-EDE1 is pseudocolored in green, MTs in red and DNA in blue. At a late stage of prophase, GFP-EDE1 appears prominently at the two poles as if forming polar caps but is undetectable in the preprophase band. At metaphase, punctate GFP-EDE1 signal overlaps largely with kinetochore fiber MTs. During cytokinesis, GFP-EDE1 is associated with two mirrored sets of phragmoplast MTs. Scale bars, 5 μm.

Figure 2. Recruitment of AUG6 to MTs by EDE1. (A) GFP-EDE1 decorates cortical MTs in a leaf epidermal cell tobacco transient expression assay. (B-D) When GFP-EDE1 (B) and AUG6-tagRFP (C) are co-expressed in a tobacco cell, AUG6-TagRFP is recruited to cortical MTs by GFP-EDE1 as demonstrated in the merged image (C). (E) Co-purification of augmin subunits as examined by mass spectrometry-assisted peptide identification. The table summarizes the number of unique (Data S1)/the number of total peptides; protein coverage by the peptides under each augmin subunit. GFP-EDE1 is used as the bait for the purification from etiolated seedlings, and AUG3-GFP was used for the purification from young flower buds and expanded leaves. Scale bar, 10 μm.

Figure 3. The *ede1-1* mutation affects MT organization during mitosis in *A. thaliana*. MTs are marked by a GFP-TUB6 fusion protein and snap shots are taken from prometaphase to cytokinesis with the time of anaphase onset designated at 0:0 (minutes : seconds) for the ease of comparison. (A) In a control cell, rigorous MT assembly leads to the formation of kinetochore fibers which appear in pairs at metaphase (from -6:54 to 0:0). Following the shortening of kinetochore fibers at anaphase (0:54), MTs become more and more prominent in the spindle midzone (2:24 and 3:18). These MTs are later developed into a bipolar phragmoplast array which expands towards the cell periphery during cytokinesis (5:06 to 14:06). (B) In an *ede1-1* cell, spindle becomes elongated and contains skewed MT bundles (-7:30 to -1:48). Anaphase onset can be judged by rapid partition or translocation of MTs towards two spindle poles (0:0 to 0:36). Afterwards, MTs are polymerized and coalesced in the spindle midzone and overall spindle length is shortened (1:48 to 3:36). A bipolar phragmoplast MT array is later developed from these MTs and the array is typically wider in the axial width compared to the control cell. Scale bar, 5 μm.

Figure 4. The *ede1-1* mutation alters γ-tubulin localization during mitosis in *A. thaliana*. Dual localizations of γ-tubulin and MTs in *ede1-1* cells at prophase, metaphase and cytokinesis. In merged images, γ-tubulin is pseudo colored in green, MTs in red and DNA in blue. In a control cell at late

prophase, γ-tubulin forms polar caps that highlight the early spindle poles. Such γ-tubulin polar caps are no longer obvious although some signals can be discerned on MT bundles formed on the nuclear envelop in an *ede1-1* cell at a similar stage. In metaphase cells, γ-tubulin is concentrated on spindle MTs in the control cell but becomes largely diffuse in the cytosol of the ede1-1 cell. During cytokinesis, γ-tubulin is concentrated on the phragmoplast MT array by biasing towards the distal ends facing daughter nuclei in the control cell. Again, the signal becomes largely diffuse and is not obviously concentrated on phragmoplast MTs in the *ede1-1* cell. Instead, prominent signal is seen on the nuclear envelope. Scale bar, 5 μm.

METHODS

CONTACT FOR REAGENT AND RESOURCE SHARING

Further information and requests for resources and reagents should be directed to and will be fulfilled by the Lead Contact, Bo Liu (bliu@ucdavis.edu).

EXPERIMENTAL MODEL AND SUBJECT DETAILS

Plant materials and growth conditions

The *Arabidopsis thaliana ede1-1* mutant was reported previously [3], and the wild-type plant with the Columbia background was used as the reference. All plants were grown in a growth chamber at 22°C with a 16-hr light and 8-hr dark cycle. For live-cell imaging, seeds were germinated on solid medium with ½ MS (Murashige & Skoog) salt mixture and 0.8% phytagel.

Transient expression experiments were carried out in leaves of the tobacco *Nicotiana benthamiana*, growing in growth chamber at 24°C with a 10-hr light and 14-hr dark cycle.

MEGHOD DETAILS

Plasmid construction

The EDE1 promoter (p):GFP-EDE1 construct was made previously [3]. The AUG3 promoter:AUG3-TagRFP was produced by the Gateway LR reaction using the pENTR-AUG3 [6] and pGWB659.

Constructs for protein expression in the tobacco leaf cells employed cDNA clones of AUG1-8, AUG8Like (AUG8L), and EDE1. The cDNA fragments were amplified using corresponding primer pairs of AUG1-8F and AUG1-8R, and EDE1F and EDE1R are listed in Table S1 by the Phusion DNA polymerase. The resulting products were digested with the restriction enzymes of NotI and AscI before being ligated with the pENTR backbone at the identical sites to give rise to pENTR-AUG1-8 and pENTR-EDE1. The final expression constructs were produced by LR recombination reactions between pENTR-AUG1-7 plasmids and pGWB660, and pENTR-AUG8/AUG8L/EDE1 and pGWB6.

To express *AUG8* under the control of the *EDE1* promoter, we use the pENTR:GFP-EDE1 as a template to amplify the EDE1 promoter plus the GFP-coding sequence using the primers of EDE1m and ENTRp. In

the meantime, the AUG8-coding sequence was amplified from its cDNA plasmid using the primers AUG8c-F and AUG8c-R. These two DNA fragments and the pENTR NotI/AscI backbone were integrated together through the Gibson reaction to produce pENTR-EDE1(p):GFP-AUG8, followed by recombination to pGWB1 in the LR reaction. The resulting pGWB1-EDE1(p):GFP-AUG8 was then transformed into the *ede1-1* mutant.

Stable transformation in *Arabidopsis thaliana*

Arabidopsis plants were transformed by the floral dip method using *Agrobacterium tumefaciens* strain GV3101. GV3101 cells carrying plasmid constructs were grown in LB media with appropriate antibiotics at 28°C for 2 days. Bacterial cells were harvested by centrifugation at 5000 rpm for 10 min, and resuspended in 5% sucrose solution containing 0.05% Silwet L-77 for Arabidopsis transformation. Transgenic plants were selected by hygromycin or BASTA depending on the plasmids used.

Transient expression in *Nicotiana benthamiana*

Transient expression experiments were carried out in leaves of the tobacco *N. benthamiana* by agrobacterial infiltration. *Agrobacterium tumefaciens* GV3101 carrying expression constructs were grown in LB media with appropriate antibiotics at 28°C for 2 days. Bacterial cells were harvested by centrifugation, and resuspended in infiltration buffer (10 mM MES pH 5.7, 10 mM $MgCl_2$, 150 μM acetosyringone). The cultures were adjusted to an OD 600 nm of 1.0, and equal volumes of cultures carrying different constructs were mixed for co-infiltration. There cells were then mixed with *A. tumefaciens* C58C1(pCH32-35S:p19) in a 1:1 ratio, followed by incubated for 3 hours at room temperature. The resulting cultures were infiltrated into leaves of 4-week-old *N. benthamiana*. The leaf samples were observed under microscope 3 days after infiltration

Immunolocalization and fluorescent microscopy

Root tips were fixed for 1 hour in 4% formaldehyde in PME (50 mM Pipes buffer, pH 6.9, 1 mM $MgSO_4$ and 5 mM EGTA). After partially digested for 30 min in 1% cellulase solution, root tip cells were released by gentle squashing onto slides coated with gelatin and chrome-alum. Following sequential treatments with 0.5% Triton X-100 for 15 min and methanol at -20°C for 10 min, the cells were processed for immunofluorescence staining. Stained cells were observed under an Eclipse 600 microscope equipped with 60X Plan-Apo and 100X Plan-Fluor objectives (Nikon) and images were acquired by an Orca CCD camera (Hamamatsu) controlled by the Metamorph software package (Molecular Devices).

To observe mitotic cell division, root tips were mounted in water before being placed under an Axio Observer inverted microscope equipped with the LSM710 laser scanning confocal module (Carl Zeiss). Cells were observed by using 40X C-Plan (water) or 63X Plan-Apo (oil) objectives, and the GFP and TagRFP signals were excited respectively by 488 and 561-nm argon laser, and images were acquired using the ZEN software package and processed in ImageJ.

In transient expression experiments, leaf segments following agrobacterial infiltration were sliced and observed under the confocal microscope described above. For the MT colocalization experiment, an RFP fusion protein with the C-terminal MT-binding domain (CTD) of the CKL6 (casein kinase 1-like 6) protein was co-expressed with the aforementioned fusion proteins in leaf cells of *N*. *benthamiana*.

Isolation of the augmin complex

To enrich GFP-EDE1 when it was expressed under the control of the 35S promoter, young etiolated seedlings were harvested for protein extraction. For AUG3-GFP, we used a transgenic line expressing the fusion protein under the control of its native promoter [6]. Young flower buds or expanded leaves were used to represent tissues with actively dividing cells or those with differentiating/differentiated cells for protein extraction. Protein purification was carried out using the µMACS GFP Isolation Kit, followed by mass spectrometry analysis in order to identify purified proteins based on the detected peptides at the Taplin Mass Spectrometry Facility, Harvard University.

QUANTIFICATION AND STATISTICAL ANALYSIS

Microsoft Excel was used to plot average of root length with standard deviations in Figure S1A, in which twenty 6-day-old seedlings were measured for each line. Percentages of deformed seeds in Figure S1B were counted from approximate 1000 seeds for each line. Spindle and cell length were measured from approximate 100 cells, and Figure S4C was plotted with the program BoxPlotR.

Supplemental Information

Figures S1, S2, S3, and S4.

Table S1. Primers used in this study. Related to Methods: Plasmid construction.

Data S1. (a). Proteins and derived peptides detected following the purification of GFP-EDE1 and associated proteins from etiolated seedlings. (b). Proteins and derived peptides detected following the purification of AUG3-GFP and associated proteins from flower buds. (c). Proteins and derived

peptides detected following the purification of AUG3-GFP and associated proteins from leaves. . Related to Figure 2E.

Movie S1. Dynamic redistribution of GFP-EDE1 during mitosis and cytokinesis in an *A. thaliana* root cell. Related to Figure 1.

Movie S2. MT reorganization during mitosis and cytokinesis in a control *A. thaliana* cell. Related to Figure 3.

Movie S3. MT reorganization during mitosis and cytokinesis in an *ede1-1* cell. Related to Figure 3.

KEY RESOURCES TABLE

REAGENT or RESOURCE	SOURCE	IDENTIFIER
Antibodies		
Rabbit anti-GFP antibodies	Thermo Fisher Scientific	A6455
Monoclonal anti-γ-tubulin antibody clone G9	[10]	N/A
Monoclonal anti-α-tubulin antibody clone DMIA	Sigma	T9026
Sheep anti-tubulin antibodies	Cytoskeleton, Inc.	ATN02
FITC-conjugated donkey anti-rabbit IgG	Rockland Antibodies & Assays	611-702-127
Texas Red–conjugated donkey anti-mouse IgG	Rockland Antibodies & Assays	610-709-124
FITC- conjugated donkey anti-mouse IgG	Rockland Antibodies & Assays	610-702-124
Texas Red–conjugated donkey anti-sheep IgG	Rockland Antibodies & Assays	613-709-168
Chemicals, Peptides, and Recombinant Proteins		
Murashige & Skoog salt mixture	ICN	2623022
Phytagel	Sigma	P8169
Hygromycin B	A.G. Scientific	H-1012-PBS
BASTA, glufosinate ammonium	Sigma	45520
Acetosyringone	Sigma	D134406
Paraformaldehyde	Electron Microscopy Sciences	15710
Cellulase RS	Karlan	2019
Critical Commercial Assays		
Phusion Hot Start II DNA Polymerase	Thermo Scientific	F549S
Gateway LR Clonase II Enzyme mix	Thermo Scientific	11791020
Restriction enzyme NotI	New England BioLabs	R0189
Restriction enzyme AscI	New England BioLabs	R0558
T4 DNA ligase	New England BioLabs	M0202
Gibson Assembly Master mix	New England BioLabs	E2611
µMACS GFP Isolation Kit	Miltenyi Biotech	130-091-125
Experimental Models: Organisms/Strains		
Arabidopsis thaliana, Columbia ecotype	ABRC	N/A
Arabidopsis thaliana, ede1-1 mutant line	[3]	N/A
Nicotiana benthamiana	Commercial Variety	N/A
Oligonucleotides		
Primers for plasmid construction	This paper	Table S1
Recombinant DNA		
pGWB1	Dr. Tsuyoshi Nakagawa, Shimane University, Japan	N/A

pGWB6	Dr. Tsuyoshi Nakagawa, Shimane University, Japan	N/A
pGWB659	Dr. Tsuyoshi Nakagawa, Shimane University, Japan	N/A
pGWB660	Dr. Tsuyoshi Nakagawa, Shimane University, Japan	N/A
AUG1 cDNA	ABRC	U21622
AUG2 cDNA	ABRC	U14982
AUG3 cDNA	Centre National de Sequencage, Evry, France	BX832241
AUG4 cDNA	ABRC	U50487
AUG5 cDNA	RIKEN BioResource Center, Ibaraki, Japan	RAFL14-35-A10
AUG6 cDNA	ABRC	U10061
AUG7 cDNA	ABRC	U90700
AUG8 cDNA	RIKEN BioResource Center, Ibaraki, Japan	RAFL09-97-J02
AUG8Like (AUG8L) cDNA	ABRC	U09601
EDE1 cDNA	Centre National de Sequencage, Evry, France	BX818775
EDE1(p):GFP-EDE1	[3]	N/A
pENTR-AUG3	[6]	N/A
pGWB4-AUG3(p):AUG3-GFP	[6]	N/A
pGWB659-AUG3(p):AUG3-TagRFP	This paper	N/A
pGWB1-EDE1(p):GFP-AUG8	This paper	N/A
pMLBART-CTD-RFP	Dr. Jung-Youn Lee, University of Delaware	N/A
p35S(p):GFP-TUB6	Dr. Takashi Hashimoto, Nara Institute of Science and Technology	N/A
Software and Algorithms		
Metamorph software package	Molecular Devices	N/A
ZEN software package	Carl Ziess	N/A
ImageJ	https://imagej.nih.gov/ij/download.html	N/A
BoxPlotR	http://shiny.chemgrid.org/boxplotr/	N/A

Figure

Click here to download Figure Lee2017R2_Figure 1.tif

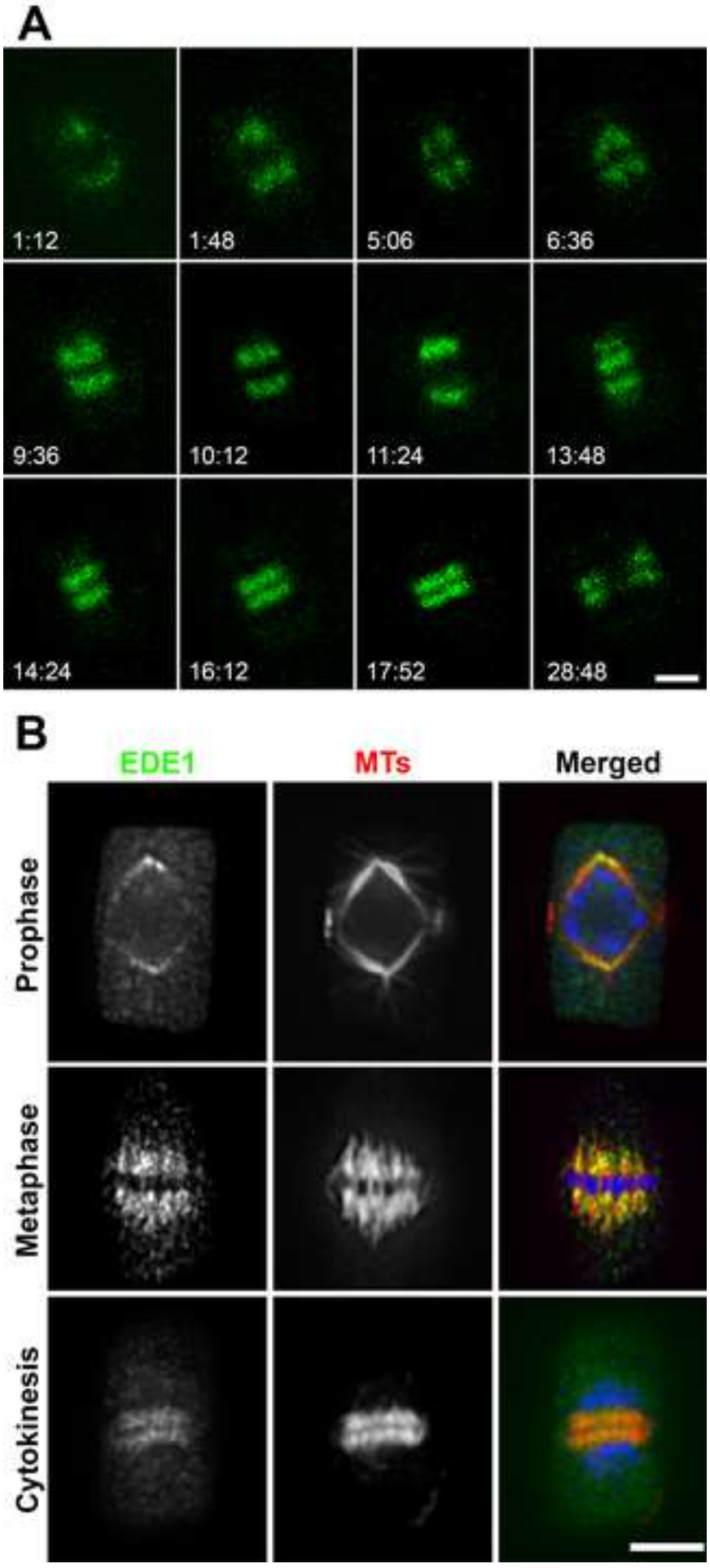

Figure

Click here to download Figure Lee2017R2_Figure 2.tif

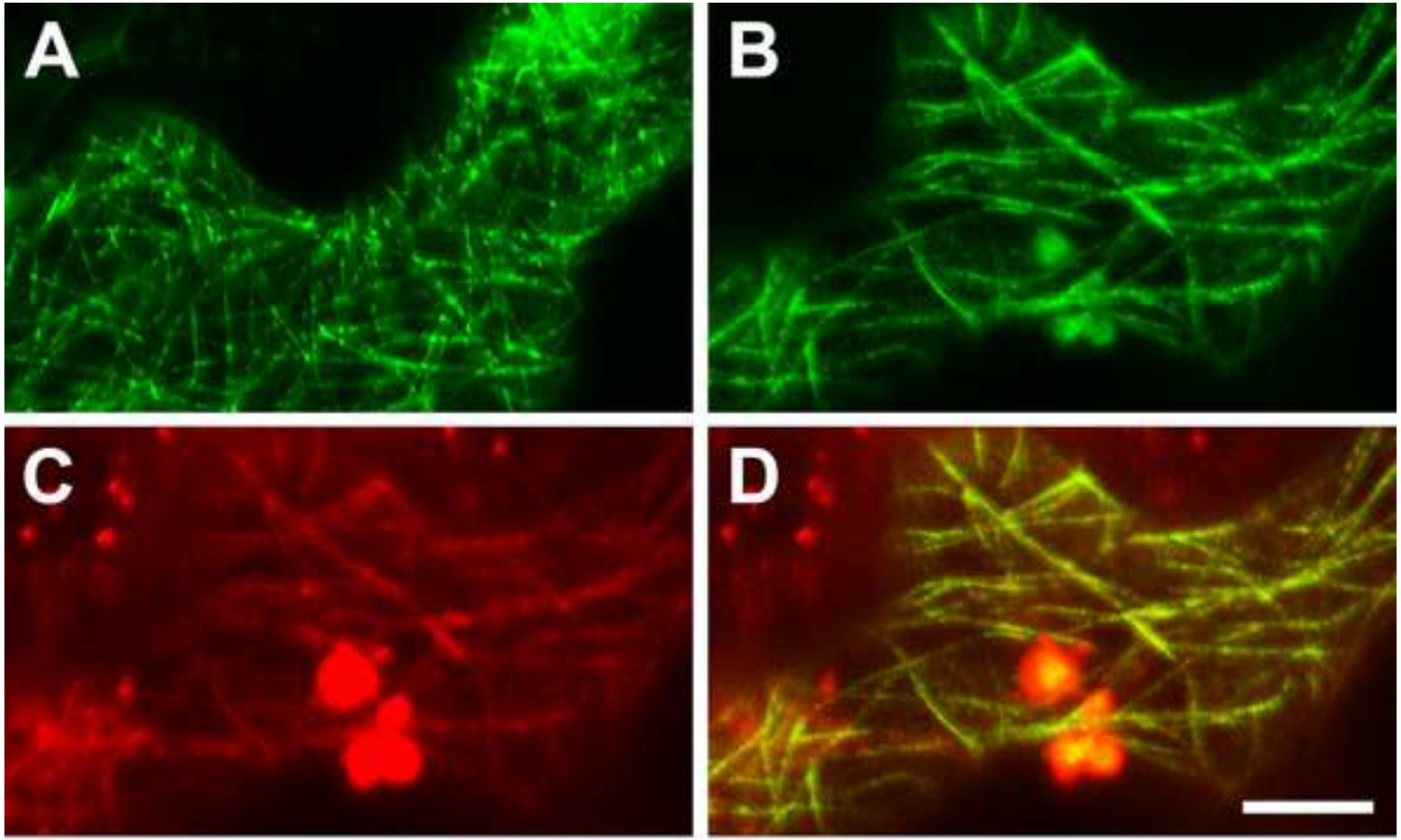

E

Detected Proteins (detected peptides and protein coverage)

Bait (source)	AUG1	AUG2	AUG3	AUG4	AUG5	AUG6	AUG7	AUG8	AUG8L	EDE1
GFP-EDE1 (seedlings)			3/3; 7.5%	3/3; 7.3%	7/7; 13.4%	5/5; 12.0%	6/6; 26.1%			1/1; 2.3%
AUG3-GFP (buds)	23/170; 59.1%	15/31; 55.7%	39/198; 51.9%	26/133; 53.2%	51/313; 64.8%	24/58; 43.3%	20/33; 76.0%	12/21; 23.9%	16/50; 31.2%	5/5; 11.8%
AUG3-GFP (leaves)	20/45; 58.4%	7/9; 28.7%	36/60; 47.7%	24/44; 51.5%	46/115; 58.4%	18/28; 37.8%	15/19; 59.0%	11/12; 26.4%	4/4; 8.4%	

Figure

Click here to download Figure Lee2017R2_Figure 3.tif

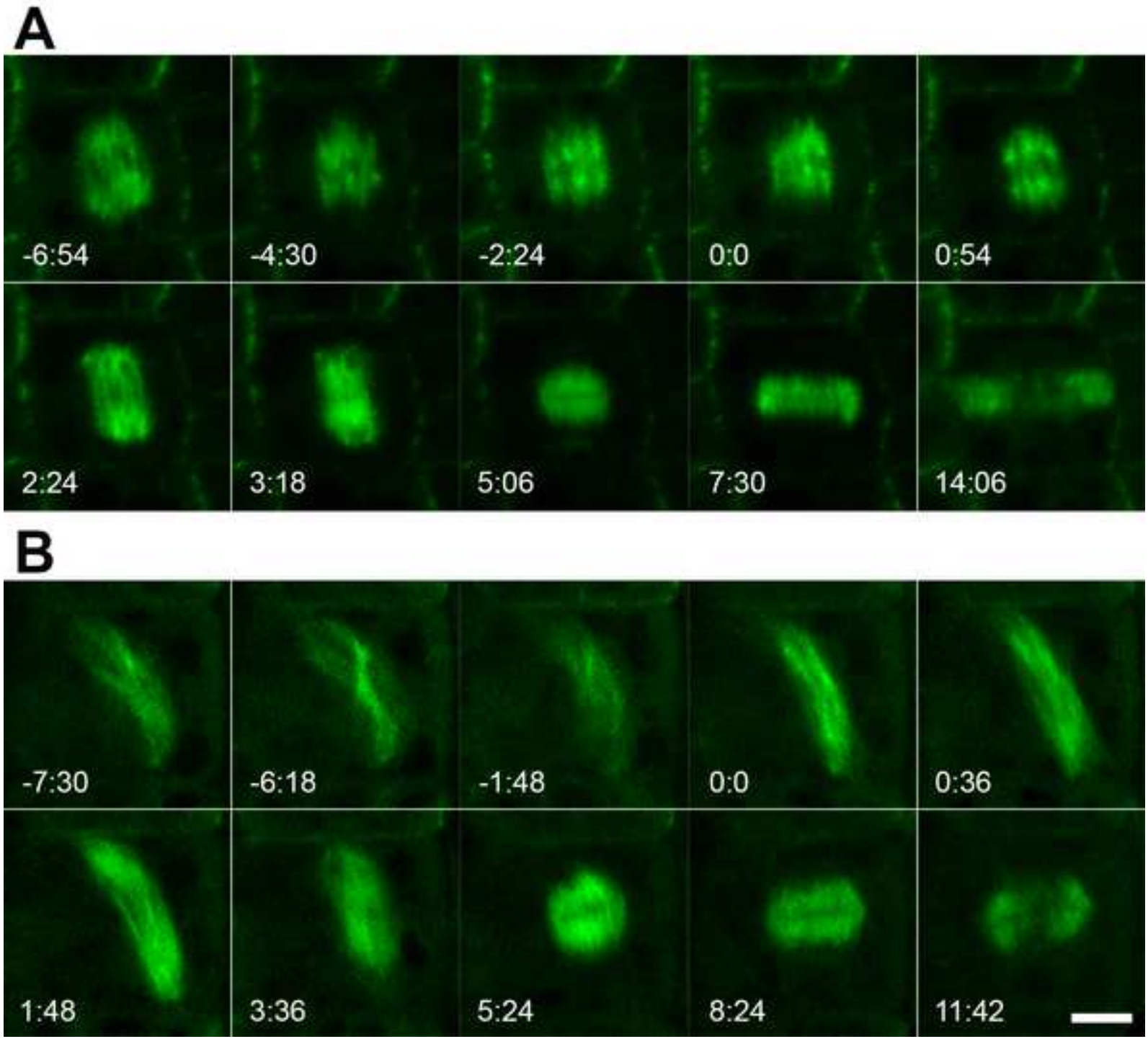

Figure

Click here to download Figure Lee2017R2_Figure 4.tif

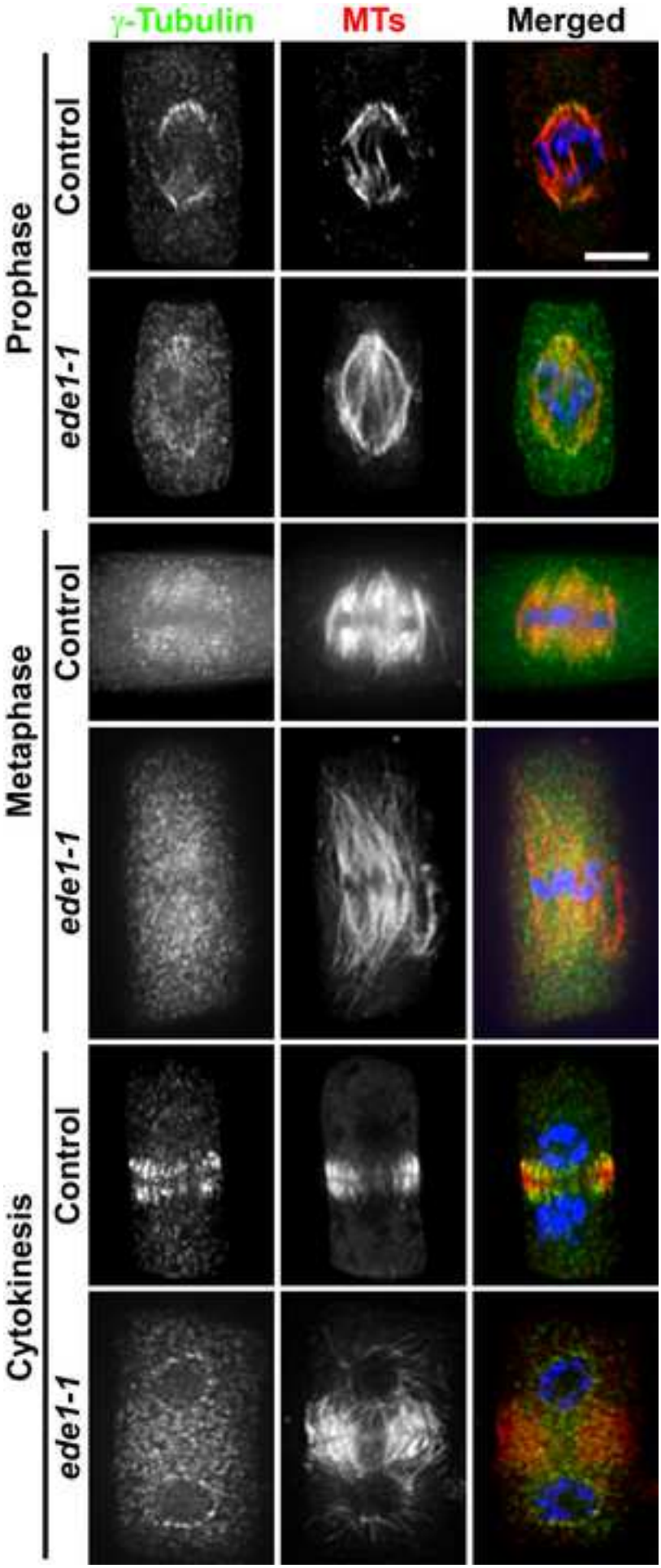

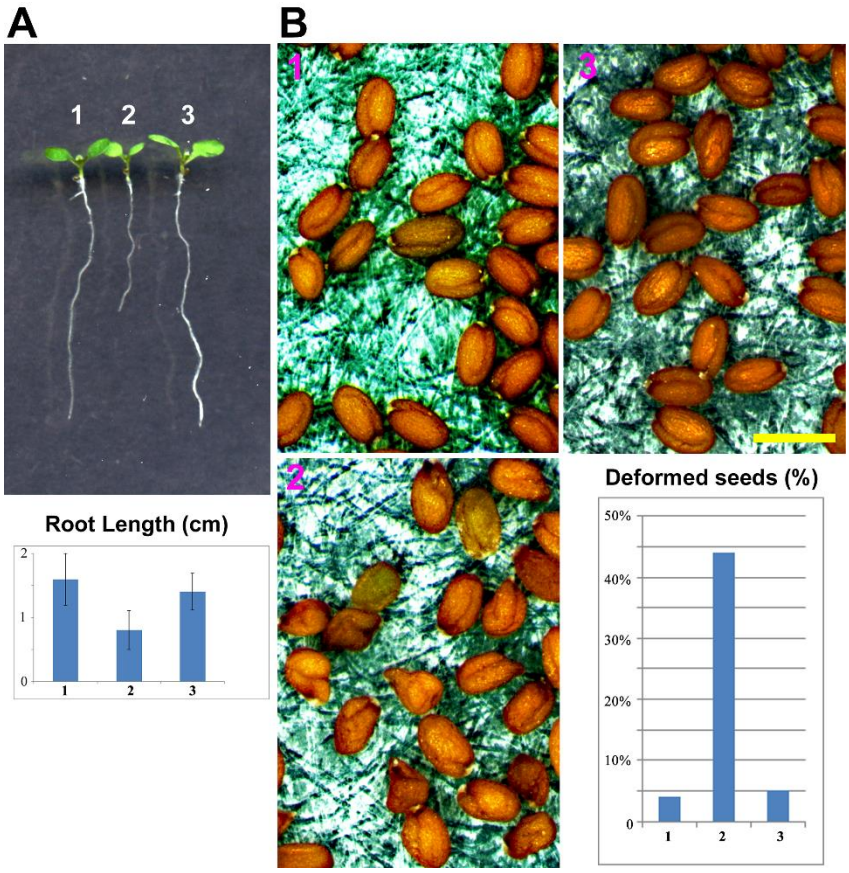

Supplemental Figure 1. **Suppression of the *ede1-1* mutation by GFP-EDE1. Related to Figure 1. (A)** The ede1-1 mutation causes retarded root growth, a phenotype fully rescued by the expression of the GFP-EDE1 fusion protein. Representative seedlings of the wild-type control (1), the *ede1-1* mutant (2), and a complemented line (3). Root lengths in cm are recorded in the accompanying chart. **(B)** Compared to the wild-type control (1), the *ede1-1* mutant produces large quantities of deformed seeds (2), a phenotype fully rescued by the expression of GFP-EDE1 (3). Percentages of deformed seeds are recorded in the accompanying chart. Scale bar, 1 mm.

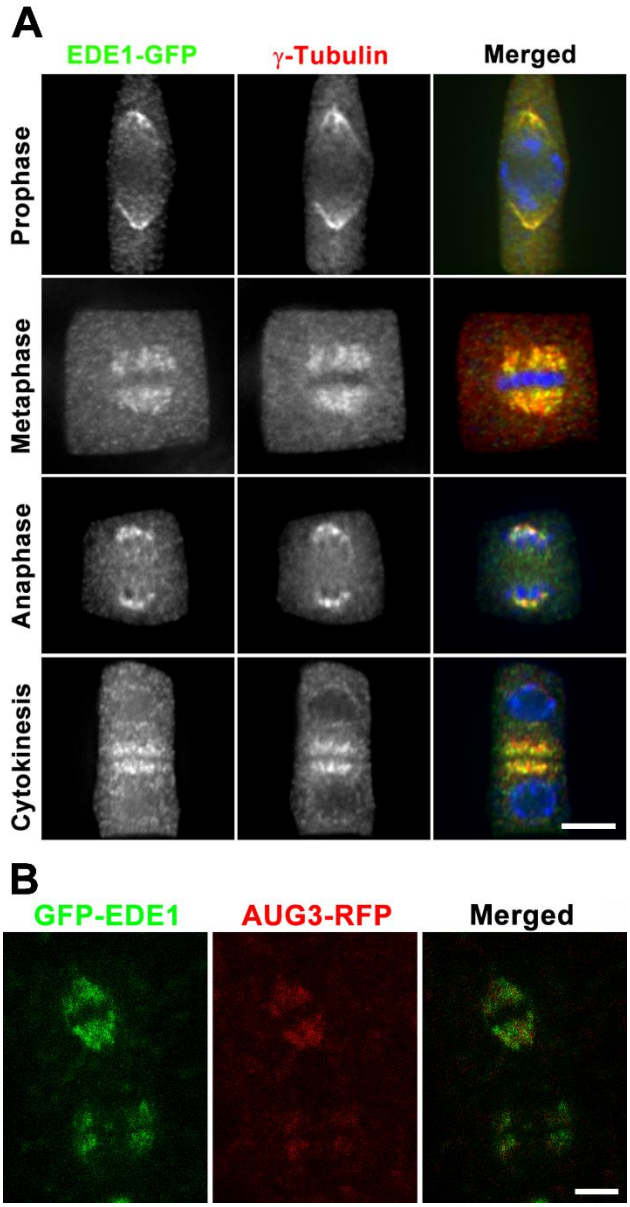

Supplemental Figure 2. Colocalization of GFP-EDE1 and other MT nucleating factors *A. thaliana* cells. Related to Figure 1. (A) GFP-EDE1 and γ-tubulin are detected by immunofluorescence in prophase, metaphase, anaphase and cytokinesis cells. The two proteins colocalize as indicated in the merged images with GFP-EDE1 in green, γ-tubulin in red, and DNA in blue. **(B)** The GFP-EDE1 and AUG3-TagRFP signals overlap completely as reflected in the merged image with GFP-EDE1 in green and AUG3-TagRFP in red. Scale bars, 5 μm.

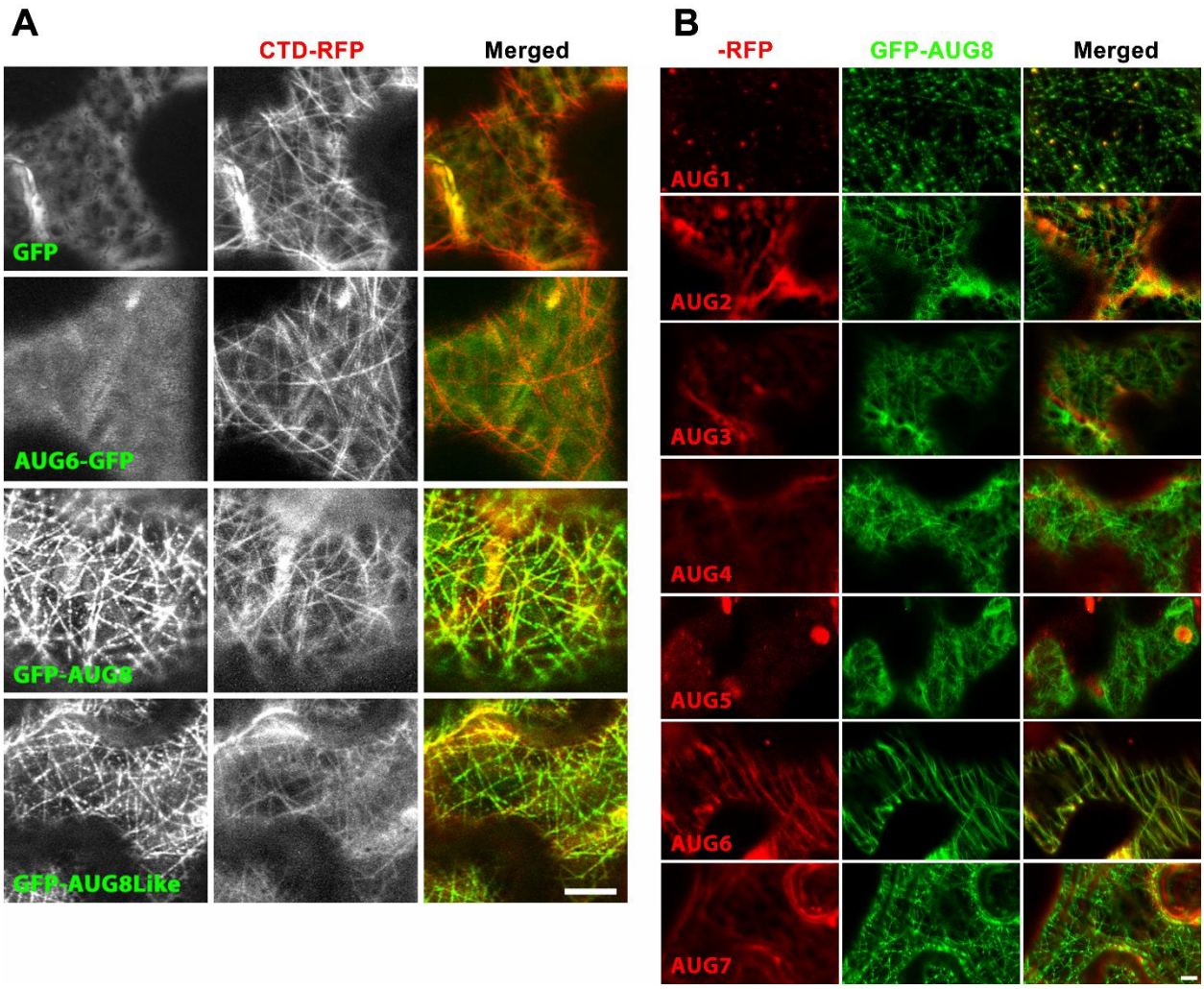

Figure 3. AUG8 family proteins are MAPs that interact with AUG6. Related to Figure 2. **(A)** Localization of AUG8 and AUG8Like proteins to cortical MTs in tobacco leaf cells. When cortical MTs are marked by the CKL6-derived CTD-RFP fusion, GFP-AUG8 and GFP-AUG8Like co-localize with the MTs as demonstrated in the merged images. In contrast, GFP alone or AUG6-GFP remain diffusely in the cytoplasm. **(B)** Recruitment of AUG6 to cortical MTs by GFP-AUG8 in tobacco leaf cells. When AUG1-7 are expressed in RFP fusion proteins together with the GFP-AUG8 fusion, AUG6 but not other AUG subunits are recruited to cortical MTs. Scale bars, 10 μm.

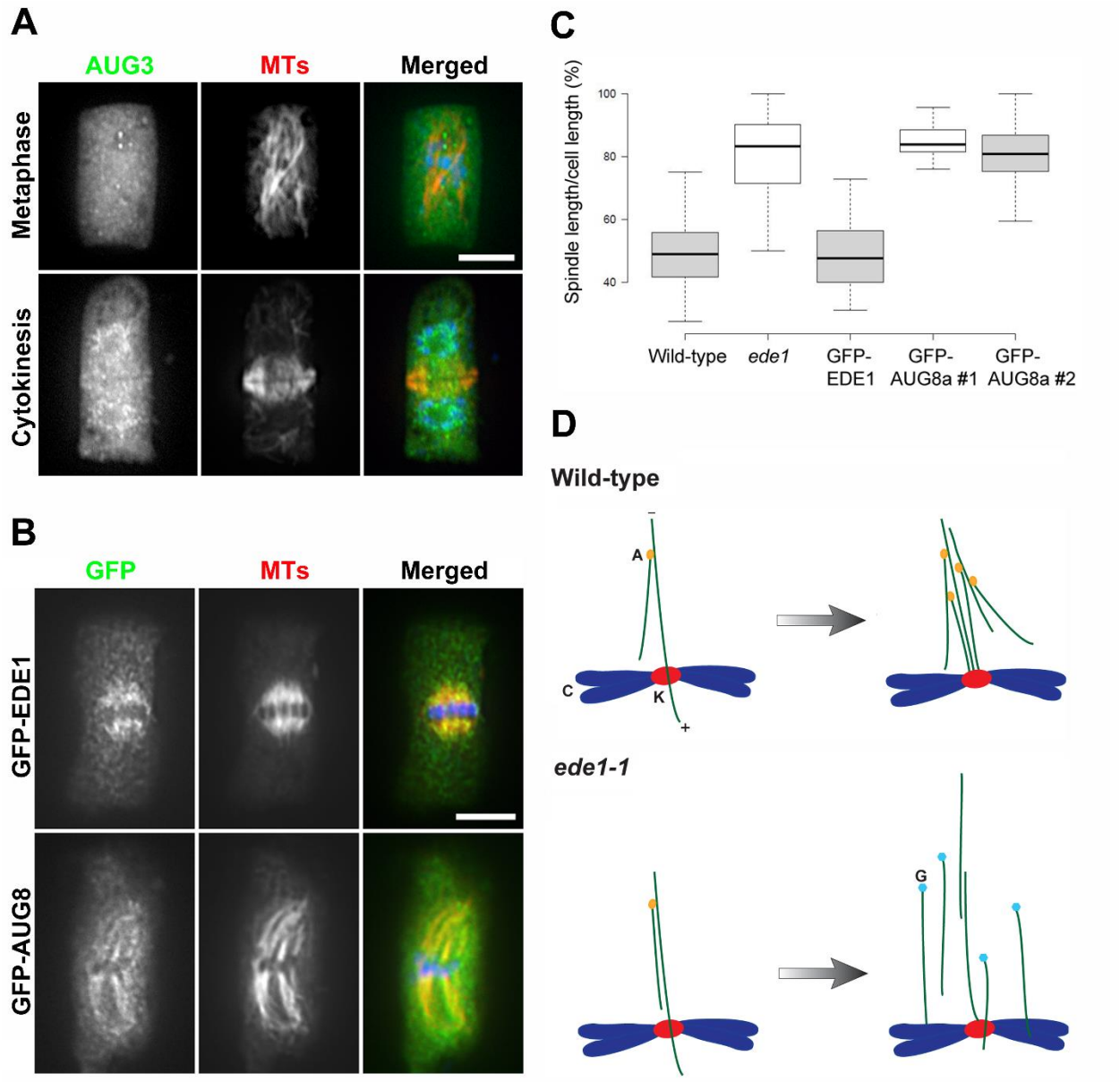

Supplemental Figure 4. The mitotic function of EDE1 cannot be replaced by AUG8. Related to Figure 4. (A) Dual localizations of AUG3-GFP and MTs in *ede1-1* cells at metaphase and cytokinesis. In merged images, AUG3-GFP is pseudocolored in green, MTs in red and DNA in blue. AUG3 localization is no longer concentrated on spindle MTs and instead becomes more or less diffuse across the cytoplasm in the metaphase cell. Such a diffuse localization pattern also can be seen when phragmoplast MTs are clearly discerned. **(B)** Dual localization of GFP-EDE1 or GFP-AUG8 and MTs in mitotic cells of transgenic lines. As demonstrated earlier, GFP-EDE1 is detected in metaphase spindles. GFP-AUG8, expressed under the EDE1 promoter, also decorates spindle MTs. **(C)** Expression of GFP-EDE1 but not GFP-AUG8 in *ede1-1* rescues the deformed spindle phenotype. Spindles from the wild-type control, the *ede1-1* mutant, a GFP-EDE1 expressing line, and two GFP-AUG8 expressing lines are assayed for their length compared to the cell length along the spindle axis. The *ede1-1* mutation causes serious spindle elongation and the EDE1 function cannot be replaced by AUG8. **(D)** Schematic diagram of MT nucleation in the wild-type and *ede1-1* mutant cells.

Green lines represent MTs with minus ends facing the pole. Chromosome arms (C) and kinetochores (K) are shown in dark blue and red, respectively. Augmin-activated nucleators (A) are highlighted in orange and augmin-independent nucleators (G) in cyan. In wild-type cells, augmin-dependent nucleation events prevail and a fir-tree like kinetochore fiber is established once more MTs are generated. In the *ede1-1* mutant, however, the branched nucleation events are largely compromised. Instead, some parallel nucleation probably takes place on extant MTs. More augmin-independent nucleation events take place in the cytosol and discrete MTs are added to the spindle. Parallel MTs may be transported or slid apart by motors so that spindles become elongated. Scale bars, 5 µm.

Click here to access/download

Supplemental Movies and Spreadsheets

Supple Video 1.avi

Click here to access/download

Supplemental Movies and Spreadsheets

Supple Video 2.avi

Click here to access/download

Supplemental Movies and Spreadsheets

Supple Video 3.avi

Click here to access/download

Supplemental Movies and Spreadsheets

Table S1.xlsx

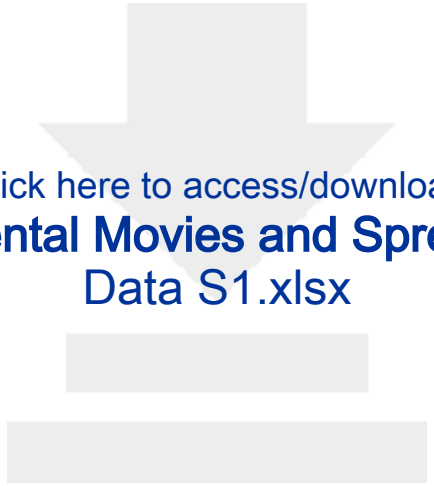

Click here to access/download

Supplemental Movies and Spreadsheets

Data S1.xlsx